Dayside open field line region boundary at high altitudes

J. F. Fennell[1], J. L. Roeder[1], R. Friedel[2], M. Grande[3], and H. E. Spence[4]

1. Space and Environment Technology Center, Aerospace Corporation, Los Angeles, CA, 90009, U. S. A.
2. Max-Planck-Institut für Aeronomie, 37191 Katlenburg-Lindau, Germany
3. Rutherford Appleton Laboratory, Chilton, Didcot, Oxon, UK
4. Boston University, Boston, MA 02215, U. S. A.

Received - September 1997 Revised - April 25, 1998 Accepted - May 5, 1998

Abstract. The Polar satellite with its high apogee and high latitude orbit offers a unique opportunity to chart the dayside open/closed field line boundary (OCB). The data from energetic particle and plasma measurements are examined to obtain the position of the OCB for a range of IMF and magnetic disturbance conditions. The Polar observations were taken within two hours of local noon in the spring and fall 1996 and spring 1997. These data were examined for evidence of IMF and solar wind control of the OCB. Some evidence of control was observed in the Polar data. However, the OCB position was found to depend more strongly on the magnetic activity levels than on IMF B_Z and solar wind pressure, for example. Examination of the invariant (Λ) and magnetic (λ) latitude of OCB for $B_Z < 1$ gave better results than using the whole data set. For $B_Z < 1$ the OCB $\Lambda \sim 78.9 + 0.38\ B_Z$ and examination of the VB_Z dependence gave $\Lambda \sim 78.9 + 1.023\ VB_Z$. The comparison with K_P gave $\Lambda \sim 80.2 - 0.88\ K_P$. These dependencies are similar to those previously observed for the auroral zone boundaries.

1 Introduction

There have been many studies of magnetospheric boundaries using both low and high altitude satellites. For example, there have been studies of the response of the cusp and the auroral oval and its boundaries to the IMF, solar wind, and magnetic activity conditions (see Hardy et al., 1981; Meng and Makita, 1986; Haerendel and Paschmann, 1982). Such studies have shown that the cusp and dayside aurora respond both to magnetic activity and external conditions.

In the present paper we attempt to identify and determine the boundary between open and closed geomagnetic field lines in the magnetosphere (hereafter denoted the OCB) with emphasis on the dayside high latitude regions. The OCB should move in much the same way as the poleward auroral and cusp boundaries discussed in the references above. The determination of the boundary between open and closed geomagnetic field lines is not an easy task and requires careful examination of the data. For example, discerning whether a field line supports particle bounce motion is not a sufficient criterion because there can be such bounce motion on open field lines which thread a region of relative magnetic field intensity minima created by localized currents such as noted by Croley et al. (1982). Flux tubes that contain isotropic particle distributions or magnetosheath plasma may indeed be closed although the particles observed appear to have exo-magnetospheric sources. It is possible for particles to leave or be attached to closed field lines because their adiabatic invariants are violated by time dependent fields (magnetic and electric) or by strong magnetic field curvature and gradients near current sheets (Alfvén, 1963).

Thus, it is difficult to label field lines as open or closed without careful assessment. We often take advantage of the fact that years of careful observations have allowed us to discern whether a particle distribution is from an exo-magnetospheric source or whether it is magnetospheric. One example of this is the soft particle fluxes observed at high latitudes of the near local noon magnetopause, i.e. the cusp/LLBL/cleft regions. The cusp, which contains magnetosheath plasma, is thought to be clearly on open field lines while the LLBL and cleft fluxes, which appear to be a mixture of unaccelerated magnetosheath and magnetospheric or accelerated magnetosheath fluxes, can exist on both open and closed field lines. Recently, Lockwood (1997) has argued that the dayside OCB should be found equatorward of the cusp if the reconnection or merged magnetosphere model is the correct picture. If that is the case, it becomes impossible to uniquely identify the dayside OCB.

However, the attempt to identify the OCB boundary is a worthwhile exercise because it is a basic concept and starting point for models of dayside solar wind magnetosphere interactions and magnetic field models. The passage of particles and energy across this boundary is a driver of magnetospheric processes. As noted above, it is expected that the position of the cusp/LLBL transition is close to and moves with the OCB (see Smith and Lockwood (1997) and Newell (1994). Using this assumption, we attempt to discern, as best we can, the position of the OCB boundary and examine its response to both external and internal conditions.

Correspondence to: J. F. Fennell

Submitted to: Journal of Physics and Chemistry of the Earth

For this paper we set as our goal to identify the OCB and determine its motions, in a statistical sense, under varying magnetic activity levels, IMF and solar wind conditions. In a later paper we plan to compare the observed OCB to the predictions of the field models such as the Tsyganenko (1990).

2 Instrumentation and Coordinates Used

For this study we used a suite of energetic particle and plasma instruments from the Polar satellite. Polar is in an approximately $2 \times 9\ R_E$ orbit at ~86° inclination with an orbital period of ~18 hours. We used data from the MICS (Magnetospheric Ion Composition Sensor), the IES and IPS (Imaging Electron and Proton Spectrometers respectively) and the Hydra plasma electron and ion sensors. The MICS measures ion fluxes in the energy range 1 - 400 keV/q and provides both ion mass and charge state identification (Wilken, et al., 1990). The IES and IPS measure the fluxes of >20 keV electrons and >18 keV protons respectively (Blake et al., 1995) over 4π sr in one satellite rotation. The Hydra DDEIS plasma sensor measures electrons and protons in the energy range ~1 to 20 keV (Scudder et al., 1995). Only spin averaged data were used for this study. The solar wind velocity and density data are from the SWE experiment (Ogilvie, 1995) on the Wind satellite while the interplanetary magnetic field (IMF) data are from MFE (Lepping, et al., 1995) on Wind. Fifteen minute running averages were made from the one minute MFE and ~90 sec SWE data for this study. The 15 minute averages were corrected for the Wind satellite position relative to the Earth.

The MICS composition measurements were used to identify the cusp by looking for intense high charge state ion fluxes with emphases on the <10 keV He^{++} and $O^{\geq 2+}$ ions. The intensity and spectra of the >1 keV H^+ from MICS and the 10 eV to 20 keV electron and proton spectra from Hydra were used to confirm the cusp and LLBL identifications. The IES and IPS were also used to help define the position of the dayside last closed drift boundary and plasma sheet boundary for energetic particles. Here, we have selected the transition from LLBL to cusp/cleft fluxes as our working definition of the OCB.

A static magnetic field model (IGRF96) was chosen for presentation of the OCB. Each Polar OCB crossing was tagged with its GSM position, invarient (Λ) and magnetic (λ) latitude and magnetic local time (MLT). The observed changes in the OCB position in Λ and λ can then be ascribed to effects such as auroral currents and interplanetary conditions. Mapping the OCB in this way does account for the motion of the Earth's dipole relative to the sun line so that, to first order, this "geometric" effect is removed.

3 Observations

An example of a boundary identification in the Polar data is shown in Fig. 1. The point chosen for our OCB boundary is identified by the vertical white line near 1240 UT and corresponds to the transition from a hotter magnetospheric plasma to an intense but colder magnetosheath plasma with high charge state ions such as He^{++} and $O^{\geq 2+}$(top two panels of

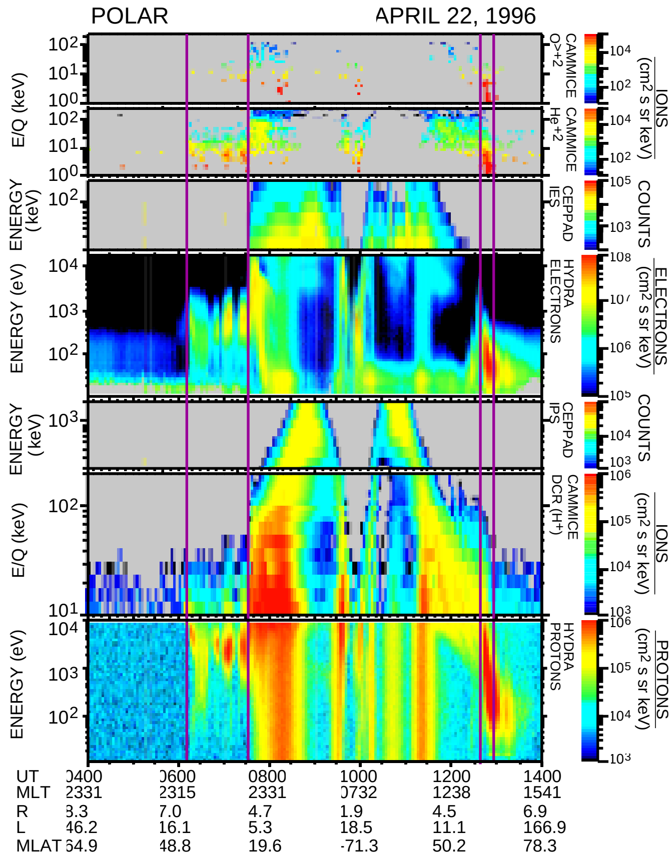

Fig. 1. MICS He++, IES, IPS, and MICS H+ spectrograms for April 22, 1996. The vertical while lines mark boundaries in the data. The boundary near 1240 UT is the OCB chosen for the dayside traversal

Fig 1). Using such identifications, we examined all the dayside high latitude crossings that occurred while Polar's orbit plane was within about two hours of the noon midnight meridian. This corresponded roughly to three different intervals (1 April - 15 May, 1996; 15 September - 15 November, 1996; 15 March - 15 May, 1997). The periods where the MICS was not operating and Wind was inside the bow shock were excluded from the study. These intervals provided 155 usable dayside crossings. We used Λ, which is a magnetic field line label like **L** , in an attempt to cast the observations into a system that is independent of the altitude of the observations. However, we show (below; Fig 4) both Λ and λ for each OCB crossing for comparison.

Figure 1 also shows a determination of the near midnight plasma sheet boundary layer (PSBL) boundary near 0615 UT. When this boundary is sharp and the polar cap above the boundary is empty of plasma ion and accelerated plasma electron fluxes (i.e. no plasma electrons other than polar rain) then we take this boundary to be the nightside polar cap or tail lobe boundary (TLB).

Because the Polar orbit is so long (~18 hr), the Polar particle data cannot be used to track the OCB motions carefully with time. These data can address the motions only in the statistical sense. Thus, it is important to know the range of magnetic activity levels and IMF and solar wind conditions that existed during the Polar observations. Fig. 2 shows the range of K_P (2a), D_{ST} (2b), IMF B_Z (2c), solar wind pressure

(P_{SW}; 2d), the solar wind speed (2e), and solar wind density (N_{SW}; 2f) that obtained for the Polar boundary crossings periods used in this study. It can be seen that there were not large numbers of extreme values and there were no large magnetic storms such as those discussed by Meng (1984). The average values of these parameters and their standard deviation for the Polar dayside crossings were $K_P \sim 1 \pm 1.2$, $D_{ST} \sim -13.5 \pm 15.5$ nT, $P_{SW} \sim 2.7 \pm 1.4$ nP, $B_Z \sim -0.1 \pm 3.2$ nT, $V_{SW} \sim 411 \pm 78$ km/sec, and $N_{SW} \sim 9.1 \pm 5.7$ cm^{-3}.

Figure 3 displays OCB and TLB (Tail Lobe Boundary: transition from tail lobe to plasma sheet boundary layer) positions in invariant latitude (Λ) versus MLT for the 155 Polar traversals used in this study. This shows that indeed the majority of dayside OCB traversals occurred within two hours of magnetic local noon because of our orbit pre-selection. The TLB data will be discussed elsewhere. We used the Λ, magnetic latitude (λ) and MLT (based on IGRF95) from the Polar ephemeris (provided by Goddard Space Flight Center) for this study. The OCB values were observed mostly in the range $75 < \Lambda < 83$ and $48 < \lambda < 68$.

Figure 4 shows scatter diagrams which contain many of the basic results for the Polar dayside crossings. We have plotted both the Λ and λ of the OCB positions against other parameters such as IMF B_Z to discern if the OCB position was controlled by or correlated with the selected parameters. The static IGRF95 field model Λ and λ values were used because they do not depend on any of the observables we compared with the OCB positions. We were primarily looking for dependencies that might be related to the IMF and solar wind conditions or magnetic activity.

Figure 4a shows the Λ and λ of the OCB plotted versus the IMF B_Z. The scatter is fairly large. The best linear fit is shown by the lines and indicates a positive dependence of the OCB Λ and λ with IMF B_Z. The coefficients of the fit and the correlation coefficient, represented by the Pierson's R value, are given in the insert on panel (a). The R value for the IMF B_Z dependence of the OCB in Λ and λ are 0.23-.27 and indicates there may be some weak relationship between the OCB latitude and B_Z. However, such small correlation coefficients are consistent with there being no correlation. We also examined the OCB Λ dependence on IMF B_X and B_Y (not shown). Both had linear fits with a slope of ~ 0.0 and very small R values (≤ 0.1) indicative of lack of correlation. The average OCB Λ and λ and their standard deviations for the 155 Polar dayside crossings were 78.5° ±1.6 and 58.4° ±5.3 respectively.

Figure 4b shows the OCB position in Λ and λ plotted versus solar wind pressure, P_{SW}. The linear fits show a negative trend with P_{SW}, indicating that the OCB latitude decreases with increased P_{SW}, as expected. However, the R value of the fits (see inset) are quite small (~ 0.16) and is probably not indicative of a real dependence of the OCB on P_{SW}. We also examined the dependence of the OCB on the components of the solar wind pressure such as the X_{GSM} component of the solar wind velocity, V_X(sw) (panel c) and the solar wind density, N_{SW} (panel d). Fig. 4d shows there was no dependence on the solar wind density with the slope of the fits near zero and the R value < 0.04. The solar wind velocity did show a trend, with Λ and λ of the OCB decreasing with increasing solar wind speed. The R value for the fits of OCB Λ and λ versus V_X were higher (~0.3) than for the P_{SW} dependence. This indicates that if there was a pressure dependence it was related more to the solar wind velocity than density.

Figures 4e and 4f show the dependence of the OCB on magnetic disturbance levels as characterized by K_P and D_{ST}. Both show a decrease in the OCB latitudes with increasing disturbance levels. The K_P and D_{ST} relationships have the largest R values and are the most believable trends in Fig. 4. Again, we point out that the range of K_P and D_{ST} for these data was relatively narrow and there were only three boundary crossings for which $K_P \geq 5$ and only two for which $D_{ST} < -50$ nT (see Fig. 2). So what Fig. 4e and Fig. 4f show is that there is a significant control of the dayside OCB latitude for very modest activity levels.

Taking a cue from the Hardy et al. (1981) study, we examined the B_Z dependence of the OCB in greater detail. Since the majority of the IMF B_Z values lie in the range $-10 < B_Z < 10$ nT, we examined the trend of Λ with B_Z over this reduced range to eliminate the few points with $|B_Z| > 10$ nT. The result is shown in Fig. 5a. Three separate linear fits are made to the data. First we fit the total data set as shown by the line marked [1]. The fit coefficients and R value are shown in the inset labeled [1]. We separately fit those points that had $B_Z < 1$ nT and $B_Z > 0$ nT as shown by the solid and dashed lines marked [2] and [3] respectively. Their coefficients and R values are shown in the insets labeled [2] and [3]. Figure 5a shows that the $B_Z < 1$ nT points (case [2]) had the strongest correlation with an R value of ~0.43. This is larger than the R value for cases [1] and [3]. The $B_Z > 0$ nT values showed no correlation with OCB Λ (case [3]) while the total data set had, at best a weak correlation. This result is similar to the results others have obtained when trying to show whether there was a relationship between dayside auroral boundaries and IMF B_Z (Hardy et al., 1981; Meng and Makita, 1986).

Because of the magnetic activity dependence observed in Fig. 4, we considered the possibility that the cross magnetosphere electric field imposed by the solar wind may be a controlling factor. Thus, we examined the variation in the OCB latitude with VB_Z (in mV/m) as shown in Fig. 5b. We restricted the OCBs to those that had $B_Z < 1$ nT and found a modest correlation with $R \sim 0.47$ and a slope of +1.023 deg/(mV/m). This would indicate that the dayside OCB has some dependence on the effective solar wind electric field. Since K_P might have a similar dependence on the solar wind electric field, we examined the K_P versus VB_Z relationship as shown in Fig. 5c. The R value is comparable to that of Fig. 5b and Fig. 4e. The Fig. 5b and Fig. 5c fits are consistent with that of Fig. 4 which indicates the OCB dependence on K_P most likely represents an OCB dependence on the solar wind electric field.

We also examined the OCB dependence on VB_Z^2 and B_Z^2 (not shown) for a solar wind energy coupling relationship and found no significant correlation. We also examined the OCB in terms of the satellite position in GSM coordinates and found that there was no organization of the data relative to any of the IMF, solar wind and distrubance parameters or the coordinates themselves (see Fennell et al., 1997). Here, they were best organized in the static magnetic field model.

4 Discussion

In a sense, the K_P and D_{ST} relationships are analogous to those obtained by Hardy et al., (1981), Gussenhoven et al, (1981) and Meng and Makita (1986) for auroral zone features. Gussenhoven et al. (1981) and Hardy et al. (1981) examined the latitude of the inner edge of the plasma sheet in relationship to K_P, IMF B_Z, solar wind speed, and solar wind electric field (VB_Z) while Meng and Makita examined the latitude of different auroral boundaries in relationship to B_Z and Meng (1984) examined the motion of the cusp in response to D_{ST}. The DMSP data set was used for those studies to obtain the auroral boundaries in corrected geomagnetic latitude. In the prenoon sector (09-10 MLT), Gussenhoven et al (1981; Table 1) found that the corrected geomagnetic latitude of the equatorward auroral boundary (Λ_{EAB}) related to K_P as $\Lambda_{EAB} \sim 69.1 - 1.64\ K_P$ which has about twice the slope we observed for the OCB vs Λ, as seen in Fig. 4e, but about 70% of the slope value we obtained for the K_P dependence versus λ. Since neither Λ nor λ is directly comparable to the corrected geomagnetic latitude used by these authors we can only say the trends are surprisingly similar given the different types of boundaries studied.

The Hardy et al. (1981) data were sparse near noon. However in the 10-11 MLT interval they obtained $\Lambda_{EAB} \sim 66.2 + 0.284\ B_Z$ for the equatorward auroral boundary with a correlation coefficient of ~0.6. This slope is within 25% of the slope of the B_Z dependence we found for the OCB in Λ and within ~30% of that in λ. In the 06-10 MLT region Meng and Makita (1986) found that the B_Z dependence of the poleward auroral boundary (Λ_{PAB}) corresponded to $\Lambda_{PAB} \sim 80.3 + 0.77\ B_Z$ with a correlation coefficient of ~0.52 which is large compared to our OCB dependence even if restricted to $B_Z < 1$ (see Fig. 5a-[1]). Meng and Makita found a slightly higher correlation (~ 0.64) if the IMF values from the hour preceding the DMSP boundary traversal were used. Both Hardy et al. (1981) and Meng and Makita (1986) found that there were better correlations with B_Z negative than for B_Z positive, consistent with expectations and also our observations of the OCB (see Fig. 5a).

The poleward auroral boundary of Meng and Makita (1986) and the cusp boundary of Meng (1984) should be more directly comparable to the results presented here. however, we observe a smaller B_Z dependence with smaller correlation coefficients, even given the different latitude systems used. We have not attempted to track the dayside OCB through magnetic storms like those of Meng (1984) because of the ~18 hr orbital period of Polar and the lack of moderate to large storms during the periods that the Polar orbit was near the noon midnight plane.

In future studies we plan to compare our results to a dynamical magnetic field model such as the Tsyganenko (1996) model and with simultaneous DMSP observations.

Acknowledgments We acknowledge the members of the instrument teams who labored long and hard to produce the high quality Polar instruments. We also thank R. Lepping and K. Ogilvie for providing the WIND data. The effort at Aerospace was supported in part under NASA grant NAG5-30368, the work at Boston University was supported in part by Aerospace subcontract 46-00000260, the effort at Max Planck Institut fuer Aeronomie was supported by contracts 50OC89131 and 50OC95022, and the work at Rutherford Appleton Laboratories was supported by the UK Particle Physics and Astronomy Research Council.

References

Alfven, H., Cosmical Electrodynamics, Oxford University Press, London, 1963.

Blake, J. B., J. F. Fennell, H. E. Spence, B. Johnson, W. A. Kolasinski, D. Mabry, J. Osborn, S. Penzin, D. N. Baker, R. Belian, T. A. Fritz, W. Ford, R. Stiglich, F. Hilsenrath, J. Kilner, J. Mobilia, H. Voss, A. Korth, M. Güll, K. Fischer, M. Grande, and D. Hall, "CEPPAD: Comprehensive Energetic Particle and Pitch Angle Distribution Experiment on POLAR", *Space Sci. Rev., 71*, 531-562, 1995.

Croley, D. R., Jr., J. F. Fennell and B. G. Ledley, Observations of Reconnection Phenomena at Synchronous Orbit, *J. Geophys. Res., 91*, 4321, 1986.

Fennell, J. F., J. B. Blake, J. L. Roeder, R. Sheldon, and H. Spence, "Tail Lobe and Open Field Line Region Entries at Mid to High Latitudes," *Adv. Space Res, 20*, 431-435, 1997.

Gussenhoven, M. S., D. A. Hardy, W. J. Burke, DMSP/F2 electron observations of equatorward auroral boundaries and their relationship to magnetospheric electric fields, *J. Geophys. Res., 86*, 768-778, 1981.

Hardy, D. A., W. J. Burke, M. S. Gussenhoven, N. Heinemann, and E. Holeman, DMSP/F2 electron observations of equatorward auroral boundaries and their relationship to the solar wind velocity and the north-south component of the interplanetary magnetic field, *J. Geophys. Res., 86*, 9961-9974, 1981.

Harendel, G. and G. Paschmann, Interaction of the solar wind with the dayside magnetosphere, in Magnetospheric Plasma Physics, 49-142, A. Nishida ed., D. Reidel Pub., Tokyo, 1982.

Lepping, R. P., M. H. Acüna, L. G. Burlaga, W. M. Farrell, J. A. Slavin, K. H. Schatten, F. Mariani, N. F. Ness, F. M. Neubauer, Y. C. Whang, J. B. Byrnes, R. S. Kennon, P. V. Panetta, J. Scheifele, and E. M. Worley, The WIND magnetic field investigation, S*pace Sci. Rev., 71*, 207-229, 1995.

Lockwood, M., Relationship of dayside auroral precipitations to the open-closed separatrix and the pattern of convective flow, *J. Geophys. Res., 102*, 17475, 1997.

Meng, C.-I., Dynamic variation of the auroral oval during intense magnetic storms, *J. Geophys. Res., 89*, 227-235, 1984.

Meng, C-I., and K. Makita, Dynamic variations of the polar cap, in Solar Wind-Magnetosphere Coupling, Kamide and Slavin eds., 605-631, Terra Scientific Co., Tokyo, Japan, 1986.

Newell, P. T., and C.-I. Meng, Ionospheric projections of magnetospheric regions under low and high solar wind pressure conditions, *J. Geophys. Res, 99*, 273-286, 1994.

Ogilvie, K. W., D. J. Chornay, R. Fitzenreiter, Hunsaker, J. Keller, J. Lobell, G. Miller, J. D. Scudder, E. C. Sittler, Jr., R. B. Torbert, D. Bodet, G. Needell, A. J. Lazarus, J. T. Steinberg, J. H. Tappan, A. Mavretic and E. Gergin, SWE, A comprehensive plasma instrument for the WIND spacecraft, *Space Sc. Rev, 71*, 55-77, 1995.

Scudder, J, F. Hunsacker, G. Miller, J. Lobell, T. Zawinstowski, K. Ogilvie, J. Keller, D. Chornay, F. Herrero, R. Fitzenreiter, D. Gairfield, J. Needel, D. Bodet, J. Googins, C. Kletzing, R. Torbert, J. Vandiver, R. Bentley, W. Fillius, C. McIlwain, E. Whipple, and A. Korth, HYDRA - A 3-dimensional electron and ion hot plasma instrument for the polar spacecraft of the GGS mission, *Space Sci. Rev., 71*, 459-495, 1995.

Smith, M. F., M. Lockwood, Earth's magnetospheric cusps, *Rev. Geophys., 32*, 233, 1996.

Tsyganenko, N. A., Quantitative models of the magnetospheric magnetic field: methods and results, *Space Sci. Rev., 54*, 75-186, 1990.

Wilken, B., W. Weiss, D. Hall, M. Grande, F. Soraas, J. F. Fennell, Magnetospheric Ion Composition Spectrometer Onboard the CRRES Spacecraft, *J. Spacecraft and Rockets, 29*, 585 (1992)